Regions of high biodiversity value preserve Nature's Contributions to People under climate change

Marta Cimatti (marta.cimatti@uniroma1.it)
La Sapienza University of Rome https://orcid.org/0000-0002-5477-4664
Rebecca Chaplin-Kramer
Stanford University https://orcid.org/0000-0002-1539-5231
Moreno Di Marco
Sapienza University of Rome

Article

Keywords:

Posted Date: September 16th, 2022

DOI: https://doi.org/10.21203/rs.3.rs-2013582/v1

Version of Record: A version of this preprint was published at Nature Sustainability on July 13th, 2023.
See the published version at https://doi.org/10.1038/s41893-023-01179-5.

Abstract

Increasing human pressures are driving a global loss of biodiversity and Nature's Contributions to People (NCP). Here, we estimated how preserving regions of high biodiversity value could reduce the risk of diminishing the provision of NCP. We analysed the impact of four different scenarios of climate change on the regulation of air quality (NCP3), climate (NCP4) and freshwater quantity (NCP6). For each indicator, we evaluated whether risk from environmental change is higher or lower within high biodiversity value regions, compared to control areas. We find higher present and future NCP levels within biodiversity regions, for all indicators. Moreover, air quality and climate regulation indicators will have higher values within biodiversity regions than outside, especially under higher emission scenarios. Understanding the spatial relationship between NCP and biodiversity, and their potential conservation synergies, is essential for sustaining human well-being and securing Earth's life support systems. Identifying the relative contribution of high biodiversity areas to NCP provision reveals potential synergies between multiple SDGs are substantial.

1. Introduction

The conservation world is at a crossroads, with ambitious conservation commitments set under the post-2021 Framework of the Convention on Biological Diversity (CBD)[1], and global health and geopolitical crises putting these commitments at risk. Yet, mounting evidence demonstrates that the conservation of biodiversity can deliver important outcomes in terms of preserving the provision of Nature's Contributions to People (NCP)[2–4]. Strategies are emerging to focus limited resources on regions of high biodiversity value that are also important for NCP to ensure that synergies between multiple environmental goals are maximized [3,5]. Yet, given rapid climate change [6] such areas might not be safe even under land protection strategies.

The Intergovernmental Science-Policy Platform on Biodiversity and Ecosystem Services (IPBES) identified 18 NCP categories organized in three partially overlapping groups: regulating, material, and non-material contributions. Regulating NCP in particular include critical ecosystem services such as pollination, regulation of water quality and climate, which outline the role of ecosystems and in determining human well-being or "good quality of life" [7]. Yet, over the past 50 years the status of all non-material and regulating NCP have declined while many material NCP (e.g. energy, food and feed, timber, medicinal resources) have increased[8,9]. Similar declining trends in regulating contributions, compared to material contributions, have also been projected for the future, under different socioeconomic development scenario [10]. Importantly, the declining trend of regulatory and non-material NCP reflects that of biodiversity, meaning these two processes are progressing in parallel.

While global biodiversity conservation can help preserve NCPs [3], rapid rates of climate change risk jeopardizing such interventions [6,11]. In fact, the effect of climate change in determining future biodiversity loss might surpass that of land-use change [9,12,13]. At the same time climate change might reduce the

availability of NCP, especially in South Asia and Africa, under the more aggressive development scenarios[14]. But can biodiversity conservation help maintain NCPs under climate change?

Measuring the current and future role of important biodiversity regions in preserving the provisioning of NCP provides insight into the potential for environmental conservation to deliver both biodiversity and NCP benefits under climate change. Recent studies have used an integrated approach of spatial conservation planning to include both biodiversity and NCP objectives, though these are limited to only few NCP indicators or focused on specific regions [3,15,16]. Crucially, none of these have investigated whether regions of high biodiversity value can play a global role in preserving NCP, and whether such role will be affected by global change.

Here we measure the importance of high biodiversity value for the maintenance of different regulating NCPs at a global scale and evaluate whether such contribution will be altered under future scenarios of climate change. We define “high biodiversity value regions” as those emerging from a comprehensive analysis of 63 published global maps, which were combined in Cimatti et al. (2021)[17] based on their underlying methodology and input data. Our goal is to estimate the avoided risk to humanity, in terms of NCP loss, that might result from conserving important biodiversity regions under global change. The IPBES Conceptual Framework makes a distinction between “potential” and “realized” NCP, where potential NCP are defined as the possibility for an ecosystem to provide an NCP independently of its demand, while the realized contribution is the actual NCP experienced or delivered, which is determined by the combination of the potential NCP and the human demand for the resulting benefits [8,9]. Since trends in potential and realized contribution usually follow the same path for regulatory NCP [9], and since future changes in population, consumption, and technology (determining realized NCP) are highly uncertain, we limit our analysis to potential NCP estimates.

We analyze different scenarios of global environmental change from the sixth Coupled Model Intercomparison Project (CMIP6), based on the five narratives developed by O’Neill et al., [18] which describe the possible combination of challenges for mitigation and adaptation to climate change. We considered four climate scenarios, from a low-emission scenario compatible with the Paris’ Goal of 2°C (scenario SSP1-2.6) to a high emission scenario that will largely fail that goal (SSP5-8.5). We evaluated the risk to the maintenance of three regulating NCP: the regulation of air quality (NCP 3), climate (NCP 4), and freshwater quantity (NCP 6). We chose seven different indicators to represent global trends in each potential NCP (Table S1) and used one representative indicator for each NCP to be reported in the main text, highlighting any discrepancy with other indicators (reported in supporting material) when present. Specifically, we used the Leaf Area Index (LAI) to represent the regulation of Air Quality (NCP 3), as the density and structural complexity of leaves determines air pollutants interception [19], the density of total carbon biomass in vegetation (cVeg) as indicator of Climate Regulation (NCP 4), and Water Availability (WA) as an indicator of Freshwater Quantity (NCP 6).

3. Results

3.1 Global trend of NCP proxies

Overall, we found an increasing global trend of both Air Quality and Climate Regulation (NCP 3 and 4, respectively) between the present and the future, while Water Quantity Regulation (NCP6) declines slightly. We found that the global mean LAI increases from 0.85 (s.d. = 0.4, among different climate models) (present value) to 0.95 (s.d. = 0.44) $m^{2/}$ m^2- 0.99 (s.d. = 0.46) $m^{2/}$ m^2 depending on the scenario (lowest under SSP1-2.6, highest under SSP5-8.5), while global mean cVeg increases from 1.85 (s.d. =0.91) kg/ m^2 to 2.16 (s.d. =0.96) and to 2.17 (s.d. = 0.94) kg/ m^2 respectively under scenarios SSP1-2.6 and SSP5-8.5. Accordingly, the mean Net Primary Productivity (NPP), an alternative climate regulation indicator shows similar trends in future scenarios. The mean global WA is projected to decline from the current − 5.6 (s.d. = 6.9) mm/month to -6.04 (s.d. = 7.2) mm/month under scenarios SSP1-2.6, and even more (-6.14, s.d. = 7.1) mm/month under scenario SSP5-8.5; this is due to actual evapotranspiration (AET) surpassing precipitation, in fact AET and the potential evapotranspiration (PET) increase under each scenario. Accordingly, the Aridity Index, an alternative indicator of freshwater regulation, reports a similar global trend.

These average global changes conceal high spatial variability in distribution of many of these NCP. While LAI (NCP 3) increases in many regions under all scenarios, extreme declines are found in Southeast Brazil, and (for SSP5-8.5) in the Gulf of Guinea and part of Tanzania (Fig. 1a and S2a). Similarly, cVeg (NCP 4) shows positive trends in almost every region, with the exception of Brazil and Central Africa, especially under the most pessimistic scenario SSP5-8.5 (Fig. 1b and S2b). In contrast, NPP increases in every region under each scenario (Fig. S3 a and b). WA (NCP 6) shows even higher spatial heterogeneity, with large declines especially in the Amazon (an area of high biodiversity value) and large increases in much of Central and Southern Africa and especially parts of China and Southeast Asia (Fig. 1c, Fig. S2c). Other indicators for water regulation show similarly heterogeneous trends, with exception of potential evapotranspiration which increases in every region apart from Central Africa and South India under scenario SSP-8.5 (see FigS3).

3.2 Effect of the high biodiversity value regions on NCP trends

In order to verify whether NCP change was significantly different inside *vs* outside high biodiversity value regions, we run a propensity score matching analysis to identify control areas with similar environmental characteristics to the biodiversity regions, within the same country. After the matching, the covariate imbalance was reduced successfully from a C-statistic value of 0.98 before the matching to 0.76 after the matching procedure (Table S5).

Most of the increases in air quality regulation, as represented by LAI, occurs within high biodiversity value regions (Fig. S1, Fig. 2). Similarly, the increases in climate regulation, as represented by carbon biomass

in vegetation, under each scenario are found within high biodiversity value regions. The mean Net Primary Productivity (NPP), also an indicator of climate regulation, shows a similar trend (see Fig. S5-S6).

Declines in mean water availability is predicted in all future scenarios and are stronger within high biodiversity value regions compared to control areas mainly due to the high risk of water loss in the Amazon, which represents the largest high biodiversity value region. Nonetheless, absolute water availability remains higher within biodiversity regions than outside under each scenario (Fig. 2, Fig. S4). Correspondingly, the mean AET and PET, also indicators of freshwater quantity, are always higher inside the high biodiversity value regions than outside under each scenario. However, while AET increases more in the future within the biodiversity regions, while PET increases are larger in control regions (see Fig. S5-S6). We found that high biodiversity value regions are less arid than control regions, both in the present and the future, however aridity will increase relatively more within the former (Fig. S5, S6).

The trend for the 10 countries with the largest extent of high biodiversity value regions generally follows the global trend across the different SSP scenarios, with greater mean changes for LAI and cVeg within the high biodiversity value regions compared to the control regions and the reverse for WA (Fig. 2-S4). However, there are some important differences in certain countries (Fig. 3, Fig. S7-S10). The greatest differences between priority and control regions are seen in Colombia Indonesia and Brazil, but where for this last one higher values of WA are found in control regions. Australia shows a smaller difference between biodiversity and control regions and Cameroon shows a strong decrease in the median value of cVeg in particular under high emission scenario SSP3-7.0 and SPP5-8.5, with a slight increase of WA under the same scenarios. These differences in NCP indicators between priority regions and control regions are always statistically significant at the country scale, with very few exceptions (Table S6). Similar results are found when selecting the top 30% high biodiversity value regions, rather than the top 10%, extending to areas located in the temperate and boreal zones of Canada and United States of America and China (Fig. S1, Fig. S11-S12).

3.2 Correlation of climate and land use change with NCP's proxies

We found that climate was always a stronger correlate of NCP change compared to land-use change, with Pearson's r values of > 0.7 between precipitation vs NCP indicators, and temperature vs NCP indicators. Instead, land-use change always had Pearson's r < 0.7 with all NCP indicators.

4. Discussion

Biodiversity loss could considerably undermine the provision of regulating and non-material NCPs [20–22] and coordinated global responses that simultaneously mitigate global change impacts on biodiversity and NCP loss are increasingly important [2,3,16,22]. While our work did not aim at establishing causality between biodiversity presence and NCP provision, we did find high spatial congruence between high

biodiversity value and high NCP provision under global environmental change both in the present and in the future.

Levels of air quality and climate regulation will increase in the future, and such increase will be higher within biodiversity regions (especially under higher emission scenarios). Water availability instead will slightly decrease in the future, especially within high value biodiversity regions. Areas of high biodiversity value in South and central America will face decreasing value of mean water availability (indicator for NCP 6), except for the Southeast coast of Brazil while on the other hand area of central Africa, Indonesia and Malaysia will be characterized by increasing WA values. High biodiversity value regions play an increasingly important role in ensuring high LAI under increasing levels of climate change (as the difference in LAI is higher under scenarios of higher emission), meaning that the conservation of these areas will be even important to preserve their air quality regulation role especially if carbon emission level will surpass the Paris targets. Our results also demonstrate that high biodiversity value regions will overlap with critical carbon sinks even if global warming surpasses 2°C above pre-industrial levels, as cVeg increases more under the two more distant scenarios, SSP1-2.6 and SSP5-8.5, compared to the others.

The discrepancies between the cVeg and LAI trends, with more consistent differences between biodiversity *vs* control areas seen in cVeg across scenarios, is probably due to a mix of factors. Changes in cVeg result from changes in NPP but also from the carbon residence time in living vegetation [23,24]. Residence time responds to CO_2 levels, which vary across scenarios, and vegetation biomass is influenced by natural disturbances, such as natural fires, which are also simulated interactively in CMIP6 for each scenario. Instead, LAI results from the carbon balance of the leaves [25,26], which is projected to increase “linearly” under each scenario (see Fig. S13). This is different from cVeg, which does not increase much under intermediate scenarios SSP2-4.5 and SSP3-7.0. This is likely related to the influence of land-use change on cVeg. In fact, while all scenarios project some increase in cropland extent, scenario SSP3-7.0 also projects substantial increase in grazing land [27]. Thus, the land use of this particular scenario is dominated by a type of vegetation with higher leaves carbon content, but lower amount of carbon stored belowground and in woody parts above ground, leading to lower total carbon in vegetation (cVeg).

The global loss of water availability under each scenario, which is even more pronounced in the high biodiversity value regions, is due to the combination of reduced precipitation and increased evapotranspiration (AET). This is especially true in the Amazon (which contains large extents of high biodiversity value regions), meaning that one of the currently most important areas for biodiversity will not be able to preserve its current freshwater quantity regulation ability in the future [28,29]. However, it is also important to recognize the contribution the evapotranspiration from the Amazon (and other extensive tropical forested regions like the Congo and Indonesia) makes in generating precipitation elsewhere. This vegetation-mediated moisture recycling accounts for a substantial portion of the

precipitation in downwind systems [30], and increased evapotranspiration in these sending ecosystems could actually increase the resilience of the receiving systems, and all the NCP they generate.

Understanding the relationship between NCP and biodiversity, and their potential conservation synergies, is essential for sustaining human well-being and securing Earth's life support systems [14,31]. Nevertheless, even as the number of studies focused on biodiversity–ecosystem-functioning relationship has increased in recent years [20,32,33], many remaining uncertainties hinder clear conclusions [21,22,34]. In fact, the relationship between biodiversity and NCP provision can be very hard to define due to the complexity of processes and interactions present in ecosystems that are seldom fully described and have remained inadequately investigated [35–37]. The fact that important biodiversity areas are strongly associated with the provision, and increase, in biomass-related NCP might be related to the fact both processes are ultimately driven by the same underlying environmental drivers. In fact, it has been found that the correlation between species richness and carbon content is higher when both variables can be independently predicted by climate, soil, and topography [31]. This is not always the case, as many open ecosystems (grasslands, savannahs) are important for biodiversity conservation but have limited carbon content; however, our delineation of high biodiversity value regions mainly include forested environments where there is high correspondence between higher diversity and higher biomass content. The pattern observed with water availability, where areas of high biodiversity value face higher risk of increased evapotranspiration than control areas, is linked to a potential overestimation of LAI, due to CO_2 fertilization effects and their impact on the hydrologic cycle. The CO_2 fertilization effects is considered the main driver of the projected increment of global LAI, which is partly offset by the negative effects of global warming, but all CMIP6 models are known to overestimate global mean LAI [38,39]. Such overestimation will lead to overestimation of carbon input to the terrestrial ecosystem (gross primary production) [40], transpiration and canopy evaporation [41]. The AET increase induced by vegetation greening through an extended area of leaves performing transpiration ,will then reduce soil moisture and runoff, which can intensify droughts at the catchment scale[42].

Analysing how the increases or decreases in potential NCP coincide with current and future human population centres is an important next step for ultimately mapping realized NCP, the actual flow of NCP that humanity receives, which could better inform policies that drive national mitigation and adaptation actions. This is especially important given the heterogeneity found in the changes in potential NCP provision between countries even within the same subregion. How future changes in population might interact with and intensify these ecological changes is a key consideration for future policy. For example, strong differences in NCP values are seen between high biodiversity value regions and control areas in Indonesia, while in Malaysia the difference is less evident. Nevertheless, population density is projected to increase strongly under all future scenarios in areas outside high biodiversity value regions in both countries, making differences in realized NCP even larger. Other countries are projected to suffer a reduction of NCP provision while population simultaneously increases: a reduction of cVeg is seen in Cameroon, Gabon, Zambia, and South Africa under various scenarios as population grows in all these countries. In contrast, despite overall declines in water quantity regulation globally, a few countries are

characterized by an increase in water availability, such as Zimbabwe, Venezuela, Suriname and Sri Lanka. In particular in these countries, both precipitation and AET decreased, but AET decreased more substantially leading to positive change of water availability (WA), while in Sri Lanka there was a higher increase of precipitation compared to the increase of evapotranspiration. Sri Lanka is also projected to go towards a major population increase compared to other countries characterized by a WA increase for which is projected a smaller increase in population. On the other hand, there are also countries such as China, where a reduction in human population will offset (to some extent) the increase of potential NCP. Thus, fully accounting for realized NCP requires an examination of not only population but demand (or need) for NCP, which may vary among countries or different social groups based on their vulnerability, and this is an important area for further work.

While both land-use change and climate change play a role in determining the change in NCP levels predicted under alternative scenarios, we found a dominant role of climate over land-use. This means that area-based conservation interventions must be coupled with bold climate mitigation policies, or risk being ineffective at preserving the crucial NCP provision role played by several important biodiversity areas. However, we found a risk of reduced water availability in these areas even under the most optimistic scenario considered in our analysis, which is compliant with the 2°C Paris target. This suggests that adaptation to climate change will assume increasing importance even under sustainability scenarios where local communities and nations will need to safeguard water resources, increase water-use efficiency, and change practices and behaviours where necessary to continue to thrive under changing precipitation patterns. Indeed, trade-offs will need to be weighed in the role of nature to provide mitigation vs. adaptation benefits for coping with climate change [43].

Spatial guidance is needed to identify areas of potential co-benefits between conserving biodiversity and NCP, in order to promote the implementation of global climate and biodiversity commitments at local levels. General conclusions have been difficult to draw from past work in which ‘biodiversity’ has generally been based on subset of global biodiversity, typically mammals and birds [44], often to the exclusion of reptiles, invertebrates and plant species, as well as other dimensions of biodiversity [3,16,31,45]. Our work synthesizes high biodiversity value regions resulting from the combination of published biodiversity conservation maps focusing on different taxa as well as phylogenetic and functional diversity [17], thus representing many different elements of biodiversity.

Our results show spatial congruence between biodiversity value and NCP value.

Regardless of whether this spatial congruence is due to correlation (via underlying environmental mechanisms) or causation, the areas we identified are important from a conservation policy perspective, allowing us to identify the relative contribution of high biodiversity value regions to NCP provision. Our results show the existence of substantial synergies between the achievement of goals set under different convention (for example, CBD and the United Nations Framework Convention on Climate Change) and different Sustainable Development Goals. Conserving areas of high biodiversity value would protect life on land (SDG15), while delivering a high contribution to good health and wellbeing (SDG3), availability of

clean water (SDG6) and mitigation of climate change (SDG 13). Thus, it is now fundamental to improve the mapping of other (less studied) NCP to understand whether other synergistic patterns (similar to those we describe here) emerge [46]. Under accelerating climate change, and under high risk of global geo-political instability from recent humanitarian catastrophes (such as COVID-19, the war in Ukraine, and many regional-scale extreme weather events) it is imperative to quickly consolidate an integrated human–nature paradigm shift incorporating NCP into the assessment of SDGs, while guiding investments and implement Nature Based Solutions for climate change adaptation and mitigation policies [47]. Here we show that spatial options for win-win strategies that achieve human and nature benefits are available, and rather substantial, and should be pursued before being eroded by human-induced environmental change.

Methods

Regulating NCP are not easily measured since different abiotic factors are intertwined in the generation of several regulating NCP. Nevertheless, the biophysical processes behind the NCP provision can be measured by evaluating different indicators. Thus, we choose different indicators to represent global trends in potential NCP when available (Table S1). We selected indicators starting from those reported in the Chap. 2.3 of the IPBES report on biodiversity and ecosystem services (IPBES 2019), and expanded the selection based on data availability across multiple climate models and multiple scenarios, following literature sources reported in the IPBES Chap. 1[9,48–51]. The data selected to evaluate the trend of different NCP were retrieved from the CMIP6 and WorldClim datasets [52,53] .We measured indicators for three NCP representing the regulation of air quality, climate, and water quantity.

We measured air quality regulation (NCP 3 under the IPBES categories) using the Leaf Area index (LAI). LAI is defined as one side of the green leaf area per unit ground area in broad leaf canopies and as one half of the total needle surface area per unit ground area in coniferous canopies [19]. LAI is used as an indicator of air quality regulation because vegetated areas with higher LAI values have a higher surface roughness, structural complexity, and density of leaves, which all contribute to intercept air pollutants and favour their further deposition and absorption [19]. Thus, a higher LAI value is associated with higher provision of NCP3.

Similarly, we used spatial estimates of the density of the total carbon (above ground and below ground) in vegetation (cVeg) as index of the climate regulation. The regulation of climate (NCP 4) depends on ecosystems through either sequestration or release of greenhouse gasses such CO2. Consequently, changes in carbon stored in vegetation can potentially mitigate warming caused by increasing concentrations of CO2 in the atmosphere [54,55].

Climate change also influences ecological processes that contribute to atmospheric carbon balance such as plant respiration and decomposition of organic matter [23], so we added the NPP to our list of indicators

for NCP4. Net primary production (NPP) is one of the main components of carbon balance and indicates the rate at which energy is stored as biomass, measuring the degree of accumulation of atmospheric CO2 into terrestrial ecosystems. NPP is equal to the difference between the carbon assimilated during photosynthesis and that released during plant respiration, thus it is an important indicator of terrestrial carbon [56].

Human and terrestrial wildlife survival relies on fresh water supply and the regulation of this contribution (NCP 6) is an essential ecosystem function. The water cycle is an extremely complex system based on different processes including precipitation, evapotranspiration, and runoff. Changes in the spatio-temporal distribution of precipitation and evapotranspiration alter the availability of water [57,58], and anthropogenic climate change affects the water balance by altering these variables [59]. Furthermore, the aridity, or the lack of moisture, depends on the same variables and many studies predicted a global terrestrial drying in the future [60–62]. Thus, in order to try to include all the different aspects characterizing the complexity of the water cycle, we choose to include in our analyses different indicators to evaluate the freshwater quantity regulation, namely the water availability (WA), the actual evapotranspiration (AET), the potential evapotranspiration (PET) and the aridity index (AI).

We reported water availability (WA) as a simple function of precipitation (P) and actual evapotranspiration (AET) [58]. WA is then expressed as the total available water that can be in the form of runoff, soil moisture, and groundwater recharge in terms of mm/month [63] as [1]:

WA = P- AET [mm/month] [1]

Data on AET and precipitation were retrieved from CMIP6 [52]. We also recalculated WA and PET index using precipitation and temperature data from WorldClim [53] as a sensitivity test to influence of data set resolution, since from WorldClim are available down scaled data at a resolution of 30s (~ 1km).

AET is defined as the actual amount of water removed from a surface area through a combined process of both evaporation from soil and plant surfaces and transpiration through plant canopies. AET is expected to increase in the future due to the warming climate and this would probably result in more frequent and intense extreme events [64]. The potential evapotranspiration (PET) can be considered as another indicator of water regulation because is a measure of the atmospheric demand for evaporation and it is independent of the supply of water itself. A higher PET value represents more arid, evaporative conditions [65] ; thus, an increase of PET would indicate a reduction of the provision of water quantity regulation (NCP6). Specifically, PET is defined as the amount of water that would potentially be removed from a vegetated surface through the processes of evaporation or transpiration when there is no water limitation, or in other words with no forcing other than atmospheric demand [66]. Many different equations have been adopted for PET estimation [67] but we chose the Hargreaves model for our study. The Hargreaves method perform almost as well as the FAO Penman–Monteith method, but required less parameterization [50]since is based only on solar radiation and temperature parameters [68] following [2]:

$PET = 0.0023* RA*(T_{mean}+17.8)*TD^{0.5}$ [mm/month] [2]

Where T_{mean} is mean monthly temperature, TD is the mean monthly temperature range and RA is the radiation on top of atmosphere.

PET can also be used to calculate a variety of aridity, drought, and soil moisture indices, as the aridity index (AI). AI is a quantitative indicator for the background climatological dryness or wetness of the land surface at given climate conditions [61], it is defined as the ratio of the mean annual precipitation to the potential evapotranspiration following [3]:

AI = P /PET [3]

Using the AI the climate of a region can be described with different five classes; hyper-arid ($AI < 0.05$), arid ($0.05 \leq AI < 0.20$), semi-arid ($0.20 \leq AI < 0.50$), dry sub-humid ($0.50 \leq AI < 0.65$), and humid ($AI \geq 0.65$).

All the AET and PET products were converted from their respective units (Kg/m^2/s and W/m^2) to millimetres per month (mm/month).

2.1 Data manipulation and calculation of trends

We collected data for the selected proxies from the CMIP6 dataset available from the archive of the earth system grid federation online system (https://esgf-node.llnl.gov/search/cmip6/) using the R package "epwshiftr" [69]. The CMIP6 dataset gathers results of many different global circulation models (GCMs) that run different experiments to simulate climates of the past, present and future. Specifically, we downloaded the data for the "historical" and the future - "SSP1-2.6", "SSP2-4.5", "SSP3-7.0" and "SSP5-8.5" - experiments. The SSP experiments represent alternative socioeconomic development scenarios, from lowest (SSP1-2.6) to highest (SSP5-8.5) levels of development intensity and hence climate change.

For each NCP indicator we use the GCMs that had data for the historical experiment and all four future experiments (Table S2). Since the spatial resolution of the different models differs, the data were resampled to a 10km grid using bilinear interpolation and re-projected into Mollweide equal-area projection. Then, the different indicators values from individual GCMs were averaged. Finally, we estimated the difference between each NCP indicator projections in the future time window (2041–2070) and the baseline period (1985–2014), under the different development scenarios (SSP1-2.6, SSP2-4.5, SSP3-7.0, and SSP5-8.5). To compare the change of different NCP, all the indicators value were rescaled between 0 and 1.

2.2 Comparing NCP projections inside and outside high biodiversity value regions

We tested whether high biodiversity value regions showed different NCP trends compared to other areas with comparable environmental characteristics. Several maps of biodiversity conservation priority have been developed in recent decades, each with partially different characteristics, built on different

approaches of spatial prioritization and different data. We represented high biodiversity value regions using the map of “biodiversity consensus” developed by Cimatti et al.[17] which synthesizes global conservation priorities and ranks regions based on their level of inclusion in independently generated biodiversity priority maps. The map of biodiversity consensus is a global map with continuous value, but we chose to report results only for the top 10% of high biodiversity value regions with the highest level of biodiversity importance covering the 10.6% of land area (Fig. S1), otherwise we would have difficulties with the propensity score matching at the country level, because there are few countries, especially in the tropics, for which almost their entire surface could be considered as a biodiversity priority region. As sensitivity test, we run the analysis for the top 30% of high biodiversity value regions which cover instead the 31.6% of land mass, excluding the countries for which it was impossible to sample control- not priority- areas (Table S4).

In order to assess the role of high biodiversity value regions at preventing decline of the NCP provision, we compared scenarios of NCP inside and outside these regions. In order to determine the effectiveness of high biodiversity value regions at retaining higher levels of NCP, it is necessary to account for the characteristics of these regions. The top-ranked high biodiversity value regions are disproportionately located in the tropics where there are usually high levels of taxonomical/phylogenetical diversity, and in wilderness areas distant from human infrastructures and urban areas, with low agricultural value [12,70]. Thus, in order to control for such selection bias, and to account for other confounding factors in biodiversity conservation priority region location, we use the propensity score matching technique [71–73] to identify areas with similar socio-environmental conditions to that of priority biodiversity regions [74]. We selected 10 bioclimatic and 3 topographic variables available from WorldClim [53], land cover variables reclassified from the European Space Agency (ESA) and a global map of accessibility describing the travel time to cities [75], all logit transformed and standardized (i.e. mean = 0; standard deviation = 1) (see table S3). Specifically, the propensity score, which is defined as the probability of receiving treatment, given the observed covariates [76], allows matching of individuals in the control and treatment conditions with the same likelihood of receiving treatment [77].We use a nearest neighbour method with a ratio 1 to 1 without replacement, such that each grid cell inside a biodiversity priority region is matched to a different non-priority grid cell with similar characteristics and within the same country. We make an exception for countries where there are not enough non-priority areas (i.e. control units) for the matching, in which case we allowed replacement in the sampling. In order to control for low- quality matches, we use a 0.25 standard deviation caliper when possible, or in other words, we select only the matches where the distance between propensity scores for treatment and controls is less than 0.25 standard deviation of the estimated propensity scores of the sample [72,77].

The highest resolution available for CMIP6 data is 100 km, while the resolution of the biodiversity priority map is 10 km; in order to avoid selecting priority and non-priority grid cells from within the same 100 km cell, we applied a filter and only selected biodiversity priority cells falling within 100km resolution grids with at least 50% consensus coverage, and we apply the same procedure to the selection of non-priority cells. We also run a sensitivity analysis to control for the effect of the filtering process using a softer

threshold, selecting 10km priority cells only if > 25% of the corresponding 100 km cell is covered by a priority region.

To assess the quality of the matching procedure, we checked for covariate balance before and after the matching, within the original dataset and in the matched sample using the C-statistic metric. This metric is given by the area under the receiver operating characteristic (ROC) curve (or C-statistic from logistic regression), from a propensity score model estimated in the matched sample [78]. The C-statistic ranges from 0.5 to 1.0 with the minimum, indicating that the propensity score model has no ability to discriminate between treated and untreated units after matching, which means perfect balance of covariates, having very similar values between the two groups [79]. Furthermore, to verify the presence of a significant difference between NCP provision within and outside high biodiversity value regions and control areas, we used the Wilcoxon signed-rank test.

2.3 Disentangling the role of climate and land use change on the effects on NCP provision.

Differently from CMIP5, CMIP6 simulations are based on a matrix that uses the shared socioeconomic pathways (SSPs, [18]) and forcing levels of the Representative Concentration Pathways (RCP) as axes. Thus, in order to investigate how well these NCP are maintained in the face of climate change, we tried to isolate the impacts of climate change from the impacts of LUC measuring the Pearson's correlation between the climate variable (mean precipitation and temperature), land use variable from Hurtt et al. 2020[27] and the NCP's indicators values from different GCMs.

References

1. Secretariat, C. B. D. *First Draft of the Post-2020 Global Biodiversity Framework*. (2021).
2. Chaplin-Kramer, R. *et al.* Mapping the planet's critical natural assets. *bioRxiv* 2020. 11.08.361014 (2022) doi:10.1101/2020.11.08.361014.
3. Jung, M. *et al.* Areas of global importance for conserving terrestrial biodiversity, carbon and water. Nat. Ecol. Evol. **5**, 1499–1509 (2021).
4. Pereira, H. M. *et al.* Global trends in biodiversity and ecosystem services from 1900 to 2050. *bioRxiv* 2020.04.14.031716 (2020) doi:10.1101/2020.04.14.031716.
5. Di Marco, M. *et al.* Synergies and trade-offs in achieving global biodiversity targets. Conserv. Biol. **30**, 189–195 (2016).
6. Loarie, S. R. *et al.* The velocity of climate change. Nature **462**, 1052–1055 (2009).
7. Díaz, S. *et al.* Assessing nature's contributions to people. Science (80-.). **359**, 270–272 (2018).
8. Brauman, K. A. *et al.* Global trends in nature's contributions to people. *Proc. Natl. Acad. Sci. U. S. A.* **117**, 32799–32805 (2020).

9. Díaz, S. *et al.* Summary for policymakers of the methodological assessment of scenarios and models of biodiversity and ecosystem services of the Intergovernmental Science-Policy Platform on Biodiversity and Ecosystem Services. Secr. Intergov. Sci. Platf. Biodivers. Ecosyst. Serv. (2019).
10. Pereira, H. M. *et al.* Global trends in biodiversity and ecosystem services from 1900 to 2050. *bioRxiv* 2020.04.14.031716 (2020) doi:10.1101/2020.04.14.031716.
11. Scheffers, B. R. *et al.* The broad footprint of climate change from genes to biomes to people. **354**, (2016).
12. Di Marco, M. *et al.* Projecting impacts of global climate and land-use scenarios on plant biodiversity using compositional-turnover modelling. Glob. Chang. Biol. **25**, 2763–2778 (2019).
13. Newbold, T. Future effects of climate and land-use change on terrestrial vertebrate community diversity under different scenarios. *Proc. R. Soc. B Biol. Sci.* **285**, (2018).
14. Chaplin-Kramer, R. *et al.* Global modeling of nature's contributions to people. Science (80-.). **366**, 255–258 (2019).
15. O'Connor, L. M. J. *et al.* Balancing conservation priorities for nature and for people in Europe. Science (80-.). **372**, 856–860 (2021).
16. Soto-Navarro, C. *et al.* Mapping co-benefits for carbon storage and biodiversity to inform conservation policy and action. Philos. Trans. R. Soc. B Biol. Sci. **375**, (2020).
17. Cimatti, M., Brooks, T. M. & Di Marco, M. Identifying science-policy consensus regions of high biodiversity value and institutional recognition. Glob. Ecol. Conserv. **32**, e01938 (2021).
18. O'Neill, B. C. *et al.* The roads ahead: Narratives for shared socioeconomic pathways describing world futures in the 21st century. Glob. Environ. Chang. **42**, 169–180 (2017).
19. Zhu, Z. *et al.* Global data sets of vegetation leaf area index (LAI)3g and fraction of photosynthetically active radiation (FPAR)3g derived from global inventory modeling and mapping studies (GIMMS) normalized difference vegetation index (NDVI3G) for the period 1981 to 2. Remote Sens. **5**, 927–948 (2013).
20. Cardinale, B. J. *et al.* Biodiversity loss and its impact on humanity. Nature **486**, 59–67 (2012).
21. Balvanera, P. *et al.* Linking biodiversity and ecosystem services: Current uncertainties and the necessary next steps. Bioscience **64**, 49–57 (2014).
22. Isbell, F. *et al.* Linking the influence and dependence of people on biodiversity across scales. Nature **546**, 65–72 (2017).
23. Friend, A. D. *et al.* Carbon residence time dominates uncertainty in terrestrial vegetation responses to future climate and atmospheric CO2. *Proc. Natl. Acad. Sci. U. S. A.* **111**, 3280–3285 (2014).
24. Pugh, T. A. M. *et al.* Understanding the uncertainty in global forest carbon turnover. Biogeosciences **17**, 3961–3989 (2020).
25. Shao, P., Zeng, X., Sakaguchi, K., Monson, R. K. & Zeng, X. Terrestrial carbon cycle: Climate relations in eight CMIP5 earth system models. J. Clim. **26**, 8744–8764 (2013).

26. Séférian, R. *et al.* Evaluation of CNRM Earth System Model, CNRM-ESM2-1: Role of Earth System Processes in Present-Day and Future Climate. J. Adv. Model. Earth Syst. **11**, 4182–4227 (2019).
27. Hurtt, G. *et al.* Harmonization of Global Land-Use Change and Management for the Period 850–2100 (LUH2) for CMIP6. *Geosci. Model Dev. Discuss.* 1–65 (2020) doi:10.5194/gmd-2019-360.
28. Runde, I., Zobel, Z. & Schwalm, C. Human and natural resource exposure to extreme drought at 1.0°C–4.0°C warming levels. Environ. Res. Lett. **17**, 064005 (2022).
29. Feng, X. *et al.* How deregulation, drought and increasing fire impact Amazonian biodiversity. Nature **597**, 516–521 (2021).
30. Keys, P. W., Wang-Erlandsson, L. & Gordon, L. J. Revealing invisible Water: Moisture recycling as an ecosystem service. PLoS One **11**, 1–16 (2016).
31. Di Marco, M., Watson, J. E. M., Currie, D. J., Possingham, H. P. & Venter, O. The extent and predictability of the biodiversity–carbon correlation. Ecol. Lett. **21**, 365–375 (2018).
32. Isbell, F. *et al.* Biodiversity increases the resistance of ecosystem productivity to climate extremes. Nature **526**, 574–577 (2015).
33. van der Plas, F. Biodiversity and ecosystem functioning in naturally assembled communities. Biol. Rev. **94**, 1220–1245 (2019).
34. Gonzalez, A. *et al.* Scaling-up biodiversity-ecosystem functioning research. Ecol. Lett. **23**, 757–776 (2020).
35. Harrison, P. A. *et al.* Linkages between biodiversity attributes and ecosystem services: A systematic review. Ecosyst. Serv. **9**, 191–203 (2014).
36. Ricketts, T. H. *et al.* Disaggregating the evidence linking biodiversity and ecosystem services. Nat. Commun. **7**, 1–8 (2016).
37. Smith, A. C. *et al.* How natural capital delivers ecosystem services: A typology derived from a systematic review. Ecosyst. Serv. **26**, 111–126 (2017).
38. Song, X., Wang, D. Y., Li, F. & Zeng, X. D. Evaluating the performance of CMIP6 Earth system models in simulating global vegetation structure and distribution. Adv. Clim. Chang. Res. **12**, 584–595 (2021).
39. Zhao, Q., Zhu, Z., Zeng, H., Zhao, W. & Myneni, R. B. Future greening of the Earth may not be as large as previously predicted. Agric. For. Meteorol. **292–293**, 108111 (2020).
40. Anav, A. *et al.* Evaluation of land surface models in reproducing satellite derived leaf area index over the high-latitude northern hemisphere. Part II: Earth system models. Remote Sens. **5**, 3637–3661 (2013).
41. Seo, H. & Kim, Y. Role of remotely sensed leaf area index assimilation in eco-hydrologic processes in different ecosystems over East Asia with Community Land Model version 4.5 – Biogeochemistry. J. Hydrol. **594**, (2021).
42. Piao, S. *et al.* Characteristics, drivers and feedbacks of global greening. Nat. Rev. Earth Environ. **1**, 14–27 (2020).

43. Chausson, A. *et al.* Mapping the effectiveness of nature-based solutions for climate change adaptation. Glob. Chang. Biol. **26**, 6134–6155 (2020).
44. Di Marco, M. *et al.* Changing trends and persisting biases in three decades of conservation science. Glob. Ecol. Conserv. **10**, 32–42 (2017).
45. Faith, D. P. *et al.* Evosystem services: An evolutionary perspective on the links between biodiversity and human well-being. Curr. Opin. Environ. Sustain. **2**, 66–74 (2010).
46. Anderson, C. B. *et al.* Determining nature's contributions to achieve the sustainable development goals. Sustain. Sci. **14**, 543–547 (2019).
47. Hole, D. G. *et al.* Make nature's role visible to achieve the SDGs. Glob. Sustain. **5**, 1–6 (2022).
48. Saatchi, S. S. *et al.* Benchmark map of forest carbon stocks in tropical regions across three continents. **108**, (2011).
49. Baccini, A. *et al.* Estimated carbon dioxide emissions from tropical deforestation improved by carbon-density maps. **2**, 182–185 (2012).
50. Trabucco, A., Zomer, R. J., Bossio, D. A., van Straaten, O. & Verchot, L. V. Climate change mitigation through afforestation/reforestation: A global analysis of hydrologic impacts with four case studies. Agric. Ecosyst. Environ. **126**, 81–97 (2008).
51. Zomer, R. J., Trabucco, A., Bossio, D. A. & Verchot, L. V. Climate change mitigation: A spatial analysis of global land suitability for clean development mechanism afforestation and reforestation. Agric. Ecosyst. Environ. **126**, 67–80 (2008).
52. Eyring, V. *et al.* Overview of the Coupled Model Intercomparison Project Phase 6 (CMIP6) experimental design and organization. 1937–1958 (2016) doi:10.5194/gmd-9-1937-2016.
53. Fick, S. E. & Hijmans, R. J. WorldClim 2: new 1-km spatial resolution climate surfaces for. Int. J. Climatol. **37**, 4302–4315 (2017).
54. Sierra, C. A., Crow, S. E., Heimann, M., Metzler, H. & Schulze, E. D. The climate benefit of carbon sequestration. Biogeosciences **18**, 1029–1048 (2021).
55. Erb, K. H. *et al.* Unexpectedly large impact of forest management and grazing on global vegetation biomass. Nature **553**, 73–76 (2018).
56. Potter, S., Randerson, T., Field, B., Matson, A. & Mooney, H. A. • IN. **7**, 811–841 (1993).
57. Dezsi, Ş. *et al.* High-resolution projections of evapotranspiration and water availability for Europe under climate change. Int. J. Climatol. **38**, 3832–3841 (2018).
58. Konapala, G., Mishra, A. K., Wada, Y. & Mann, M. E. Climate change will affect global water availability through compounding changes in seasonal precipitation and evaporation. Nat. Commun. **11**, 1–10 (2020).
59. Guo, D., Westra, S. & Maier, H. R. Sensitivity of potential evapotranspiration to changes in climate variables for different Australian climatic zones. Hydrol. Earth Syst. Sci. **21**, 2107–2126 (2017).
60. Wang, X., Jiang, D. & Lang, X. Future changes in Aridity Index at two and four degrees of global warming above preindustrial levels. Int. J. Climatol. **41**, 278–294 (2020).

61. Park, C. E. *et al.* Keeping global warming within 1.5 °c constrains emergence of aridification. Nat. Clim. Chang. **8**, 70–74 (2018).
62. Lin, L., Gettelman, A., Fu, Q. & Xu, Y. Simulated differences in 21st century aridity due to different scenarios of greenhouse gases and aerosols. Clim. Change **146**, 407–422 (2018).
63. Tadese, M., Kumar, L. & Koech, R. Long-term variability in potential evapotranspiration, water availability and drought under climate change scenarios in the Awash River Basin, Ethiopia. Atmosphere (Basel). **11**, (2020).
64. Nooni, I. K. *et al.* Future changes in simulated evapotranspiration across continental africa based on cmip6 cnrm-cm6. Int. J. Environ. Res. Public Health **18**, 1–17 (2021).
65. Liu, X., Li, C., Zhao, T. & Han, L. Future changes of global potential evapotranspiration simulated from CMIP5 to CMIP6 models. Atmos. Ocean. Sci. Lett. **13**, 568–575 (2020).
66. Allen, R. G., Pereira, L. S., Raes, D. & Smith, M. FAO Irrigation and Drainage Paper No. 56 - Crop Evapotranspiration. (1998).
67. Zarei, A. R. & Mahmoudi, M. R. Assessment of the effect of PET calculation method on the Standardized Precipitation Evapotranspiration Index (SPEI). Arab. J. Geosci. **13**, (2020).
68. Hargreaves, G. H. Defining and using reference evapotranspiration. J. Irrig. Drain. Eng. **120**, 1132–1139 (1994).
69. Jia, H. & Chong, A. epwshiftr: Create Future 'EnergyPlus' Weather Files using 'CMIP6' Data. R package version 0.1.3. (2021).
70. Mittermeier, R. A. *et al.* Wilderness and biodiversity conservation. *Proc. Natl. Acad. Sci. U. S. A.* **100**, 10309–10313 (2003).
71. Ho, D. E., Imai, K., King, G. & Stuart, E. A. Matching as nonparametric preprocessing for reducing model dependence in parametric causal inference. Polit. Anal. **15**, 199–236 (2007).
72. Negret, P. J. *et al.* Effects of spatial autocorrelation and sampling design on estimates of protected area effectiveness. Conserv. Biol. (2020) doi:10.1111/cobi.13522.
73. Stuart, E. A. Matching Methods for Causal Inference: A Review and a Look Forward. **25**, 1–21 (2010).
74. Schleicher, J. *et al.* Statistical matching for conservation science. **00**, 1–12 (2019).
75. Weiss, D. J. *et al.* inequalities in accessibility in 2015. Nat. Publ. Gr. **553**, 333–336 (2018).
76. Stuart, E. A., Lee, B. K. & Leacy, F. P. Prognostic score e based balance measures can be a useful diagnostic for propensity score methods in comparative effectiveness research. *JCE* **66**, S84-S90.e1 (2013).
77. Olmos, A. & Govindasamy, P. Propensity Scores: A Practical Introduction Using R. J. Multidiscip. Eval. **11**, 68–88 (2015).
78. Stürmer, T. *et al.* A review of the application of propensity score methods yielded increasing use, advantages in specific settings, but not substantially different estimates compared with conventional multivariable methods. *J. Clin. Epidemiol.* **59**, 437.e1-437.e24 (2006).

79. Franklin, J. M., Rassen, J. A., Ackermann, D., Bartels, D. B. & Schneeweiss, S. Metrics for covariate balance in cohort studies of causal effects. Stat. Med. **33**, 1685–1699 (2014).

Figures

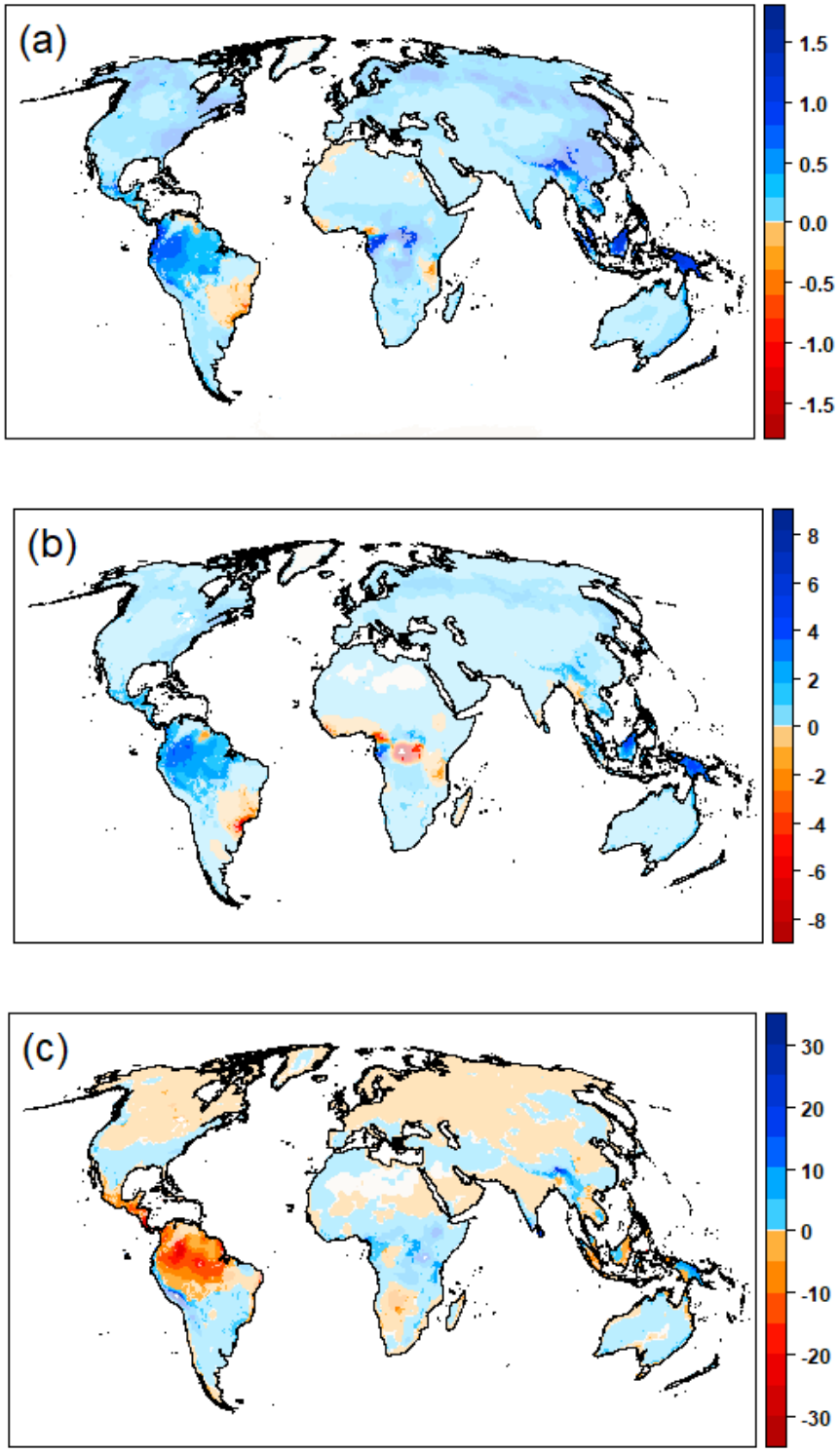

Figure 1

Projections of change in the value of Nature's Contributions to People (NCP) between the baseline period 1985-2014 and the future 2041-2070, under scenario SSP5-8.5. The panels report the absolute change in levels of three NCP indicators: (a) NCP3 represented by Leaf Area Index (LAI), in m2/m2; (b) NCP4 represented by total carbon biomass in vegetation (cVeg), in kg/m2; (c) NCP6 represented by Water Availability (WA), in mm/month. Masked opaque areas indicate regions outside the top 10% biodiversity conservation priorities. See Fig. S2 for scenario SSP1-2.6 and Fig. S3 for other indicators. Regions of high biodiversity value are indicated in Fig. S1.

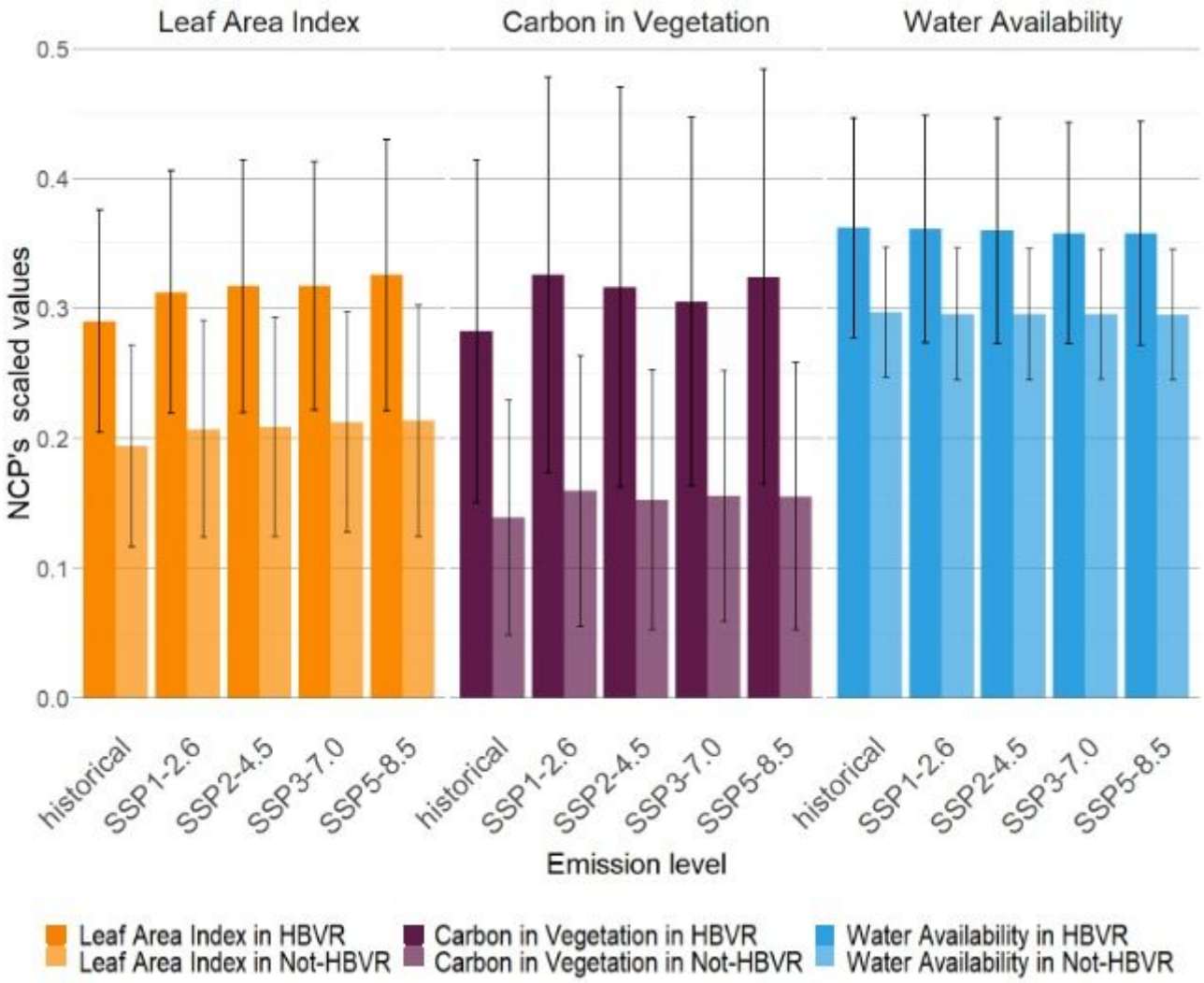

Figure 2

Barplots of the levels of three NCP indicators in the baseline period and under different future scenario for the year 2050. Indicators are reported separately for areas inside the top 10% high biodiversity value regions(HBVR) and control areas (Not-HBVR).

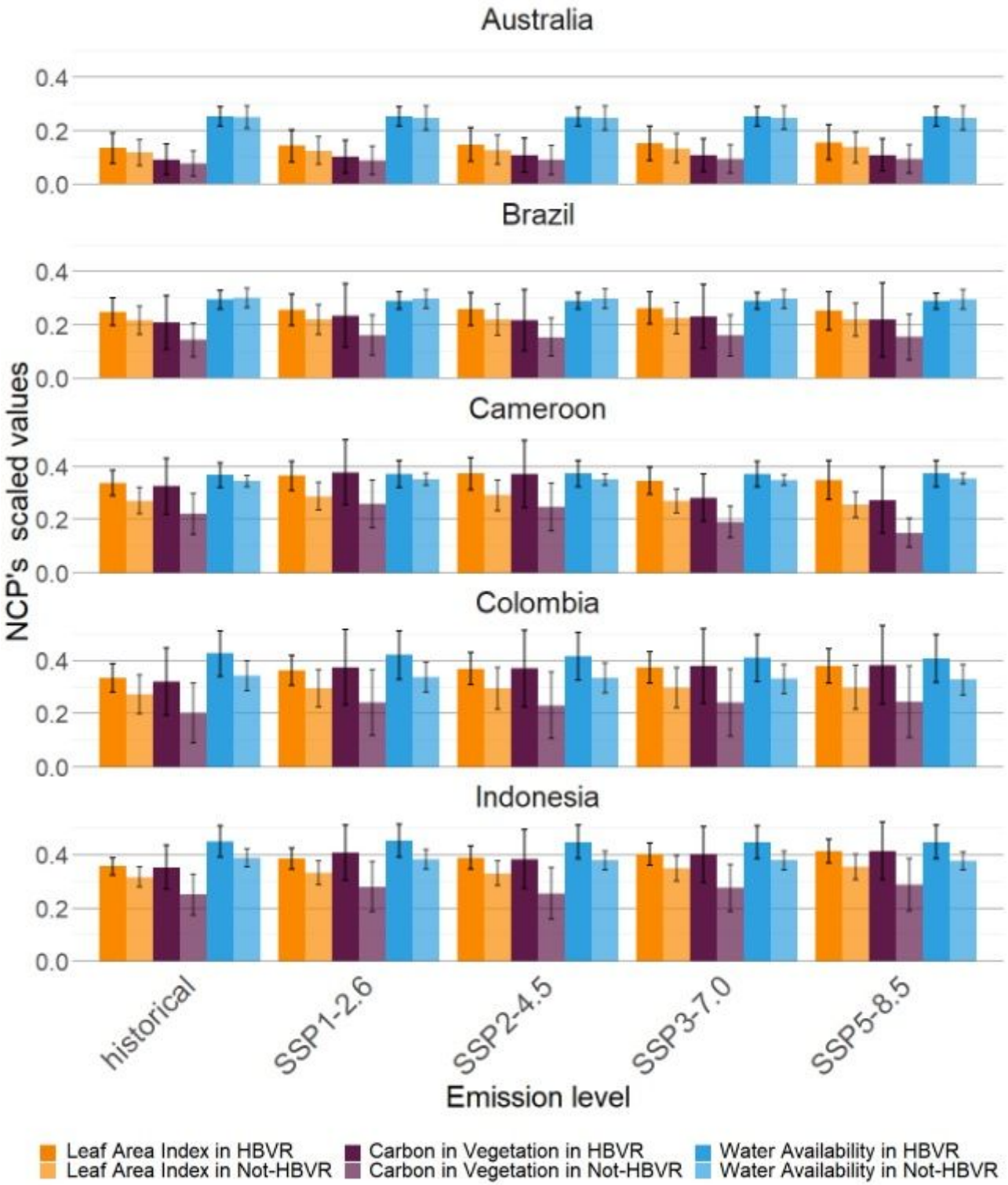

Figure 3

Barplots of the levels of three NCP indicators in the baseline period and under different future scenario for the year 2050. Indicators are reported separately for areas inside the top 10% high biodiversity value regions (HBVR) and control areas (Not-HBVR). Separate plots are reported for the five countries with the highest coverage of high biodiversity value regions (representing four continents).

Supplementary Files

This is a list of supplementary files associated with this preprint. Click to download.

- SUPPLEMENTARYINFORMATION.pdf